

High-gain Mechanically Amplified Capacitive Strain Sensor

Jun Guo, Michael Suster, Darrin J. Young, and Wen H. Ko
 Electrical Engineering and Computer Science Department
 Case Western Reserve University
 Cleveland, OH, 44106, USA
 Jxg77@po.cwru.edu

Abstract— A novel concept of mechanical amplification using buckled beam suspensions and packaging has been demonstrated in capacitive strain sensor design for improved sensitivity. However, the mechanical gain structure introduces a nonlinear characteristic, which degrades the device’s linearity. A 6% nonlinearity was observed at 1000 micro-strain. Therefore, further research efforts are required for improvements. This paper presents an in-depth study of the buckled beams characteristics on nonlinearity analytically and by FEA. The accuracy of the modeling is verified by the measurements. The analysis results show the tradeoff between mechanical gain and linearity, and can be improved by device geometrical optimization. Furthermore, the accuracy of the modeling results in predictable device characteristics, allowing the development of a 2nd order nonlinear electronic compensation method to achieve an overall system performance. Simulation results show that, by applying this technique, the overall system nonlinearity can be greatly reduced from 6% FS to 0.2% FS.

A fabricated device in Fig. 2 demonstrated a differential mechanical gain around 10 under strain from -1000 $\mu\epsilon$ (tensile) to +1000 $\mu\epsilon$ (compressive). Combined with a custom designed matching interface circuit, a capacitance to voltage converter, the overall system achieved a resolution of 0.1 microstrains ($\mu\epsilon$) and 81 dynamic range over 10 kHz bandwidth [2]. However the test results also show device’s nonlinear characteristics. Using the linear fitting method, the device shows an overall 5% nonlinearity, which motivates an in-depth nonlinearity study and modeling of the device for further improvements.

I. INTRODUCTION

A novel capacitive strain sensor employing the concept of mechanical amplification using buckled beam suspensions was demonstrated for improved sensitivity [1]. Fig. 1(a) shows the principle of the buckled beam amplification scheme: a small lateral displacement, Δx , generated by an input strain, can introduce a large center deflection of the beam, Δw , thus resulting in a mechanical gain. The differential capacitive output can be obtained by designing comb drive fingers at the structural center, as shown in Fig. 1(b).

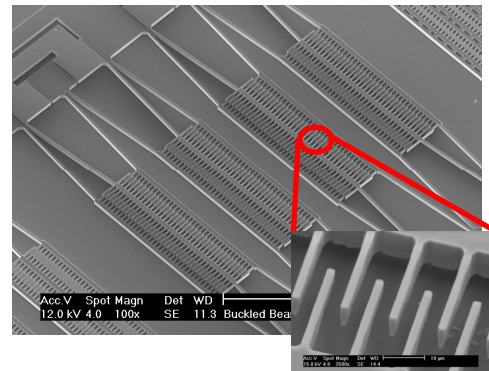


Figure 2. An SEM picture of a fabricated buckled beam capacitive strain sensor (may not be important).

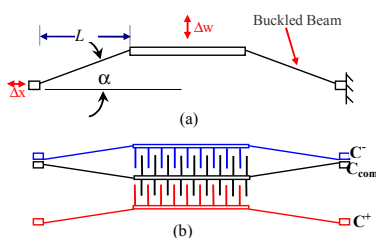


Figure 1. Principle of a buckled beam amplification scheme.

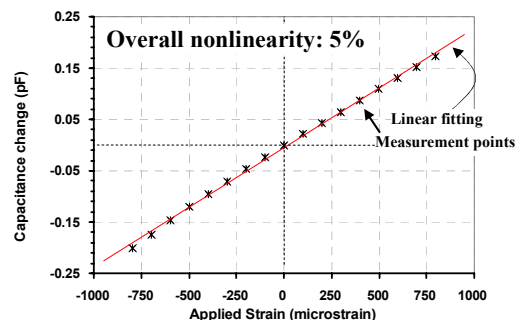


Figure 3. Measured characteristics of a 1st generation device.

II. MODELING

An analytical analysis based on the simple beam theory was developed to predict the mechanical gain of the buckled beam [3]. The sensor structure can be simplified as a simple beam structure constrained as shown in Fig. 4(a) with one end fixed and the other end guided along the x-axis. The forces acting on the bent beam are shown in Fig. 4(b), where F is the equivalent force applied by the external strain, M_o is moment from the fixed end, M is the moment in the beam at an arbitrary location (x,y) , and the governing equation is given by [4],

$$EI \frac{d^2 y}{dx^2} = M_o = M - Fy, \quad (1)$$

where E and I are the Young's modulus and moment of inertia of the beam, respectively.

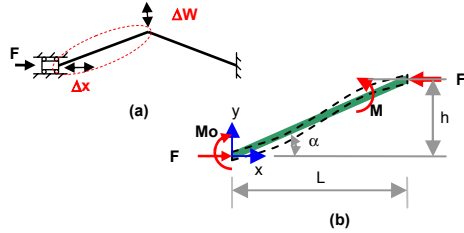


Figure 4. (a) The simplified structure. (b) Forces acting on the beam.

The boundary conditions are given by,

$$y|_{x=0} = 0, \quad \frac{dy}{dx}|_{x=0} = \tan \alpha, \quad \text{and} \quad \frac{dy}{dx}|_{x=L} = \tan \alpha. \quad (2)$$

By solving the above equations, and assuming that the changes of angle, α , can be neglected, the center deflection, Δw , can be expressed by,

$$\Delta w = 2 \frac{\tan \alpha}{k} \tan(kL/2) - h, \quad (\text{compression}) \quad (3a)$$

$$\Delta w = 2 \frac{\tan \alpha}{k} \tanh(kL/2) - h, \quad (\text{tension}) \quad (3b)$$

where $k = \sqrt{F/EI}$.

The end displacement of the buckled beam can be calculated by,

$$\Delta x = \int_0^L \frac{1}{2} \left(\frac{dy}{dx} \right)^2 dx - L \frac{1}{2} \tan^2 \alpha, \quad (\text{compression}) \quad (4a)$$

$$\Delta x = \int_0^L \frac{1}{2} \left(\frac{dy}{dx} \right)^2 dx - L \frac{1}{2} \tanh^2 \alpha. \quad (\text{tension}) \quad (4b)$$

Therefore, the mechanical gain of the buckled beam can be obtained as,

$$A_{mech} = \frac{\Delta w}{\Delta x} = \frac{2 \frac{\tan \alpha}{k} \tan(kL/2) - h}{\tan^2 \alpha \left[\frac{\tan^2(kL/2)}{4k} (-\sin(2kL) + 2kL) + \frac{\sin(2kL) + 2kL}{4k} - \frac{\tan(kL/2)}{2k} (\cos(2kL) - 1) \right]}, \quad (\text{compression}) \quad (5a)$$

$$A_{mech} = \frac{\Delta w}{\Delta x} = \frac{2 \frac{\tan \alpha}{k} \tanh(kL/2) - h}{\tan^2 \alpha \left[\frac{\tanh^2(kL/2)}{4k} (\sinh(2kL) - 2kL) + \frac{\sinh(2kL) + 2kL}{4k} - \frac{\tanh(kL/2)}{2k} (\cosh(2kL) - 1) \right]}. \quad (\text{tension}) \quad (5b)$$

For a small load Δx , the mechanical gain of the buckled beam can be simplified as,

$$A_{mech_nom} = \frac{1}{2 \tan \alpha}, \quad (6)$$

which is defined as the structure nominal gain.

For a large load, the beam buckling angle changes with the load that introduces the device's nonlinear characteristics. When the device is under a tensile strain, the buckling angle tends to decrease, which results in an increased mechanical gain. On the other hand, when the device is under compressive strain, the buckling angle tends to increase, which results in a decreased mechanical gain. A modified equation from (6) can be derived by replacing α with $\alpha + \Delta\alpha$, where $\Delta\alpha$ equals to $\Delta x / (\tan \alpha \cdot L)$ and the modified equation is obtained by applying a first-order approximation:

$$A_{mech}^* = \frac{1}{2 \tan \alpha} \left[1 - \frac{1}{2 \tan^2 \alpha} \frac{\Delta x}{L} \right]. \quad (7)$$

An FEA analysis using ANSYS was performed to verify the results of above analysis. The beam structure under analysis has geometrical parameters such as $L=300 \mu\text{m}$, $h=30 \mu\text{m}$, $\alpha=5.7^\circ$, beam width= $6 \mu\text{m}$, material Young's modulus of 130 GPa and Poisson's ratio of 0.3. The structure is under maximum load Δx of $\pm 1 \mu\text{m}$ with equivalent maximum $\Delta x/L$ of 3333×10^{-6} . Fig. 5 shows the comparison of mechanical gain obtained analytically by (5,6,&7), and by FEA. Compared to the FEA results, Eq. (5) gives the closest match with a maximum discrepancy of 0.7%, while (6) gives the least match with a maximum discrepancy around 10%. Eq. (7) shows a maximum discrepancy of 2.0%, which is accurate enough for most of the applications.

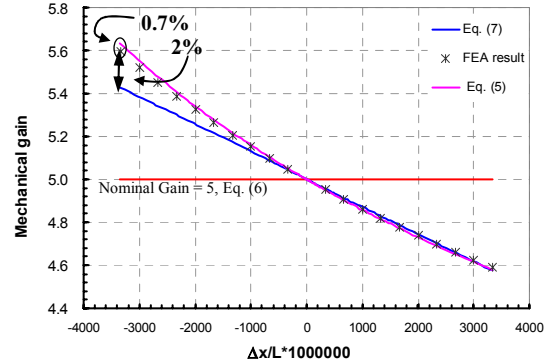


Figure 5. Comparison of mechanical gain obtained analytically by (5-7), and by FEA.

The above derived equations show the nominal mechanical gain is determined by the buckling angle and large gain is achieved by small buckling angle. The analysis results also reveal that there are tradeoffs between sensor linearity, sensitivity (mechanical gain), and operation range ($\Delta x/L$). The analysis also give me ways to improve the device overall performance by altering the structure or employing optimized geometrical parameters.

Structure improvement

Fig. 6 shows an altered structure for improved sensitivity and linearity. Instead of designing comb drive sensing fingers on the structure center, as shown in Fig. 6(a), the improved structure, as shown in Fig. 6(b) minimizes the central structure width and attaches a separate beam at the center joint of two buckle beams to accommodate the sensing fingers. Obviously, more fingers can be accommodated to achieve improved sensitivity. The two structures have the same buckling angle and gauge length (L_g); thus if under the same strain, they generate the same displacement load, Δx . However, as they have different buckling beam lengths, L_b , linearity improvements using structure (b) can be expected according to (7). Structure (b) does have one dis-advantage, that is the structure has lower mechanical resonant frequency as more mass was added to the structure. Therefore, FEA analysis is used to select the structure geometrical parameters such as beam width to satisfy the mechanical resonant requirements.

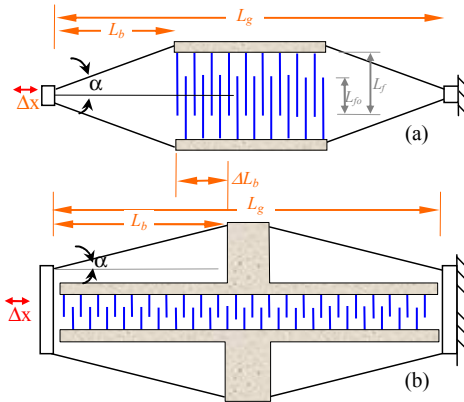


Figure 6. Structure improvements.

Parameter optimization

Fig.7 shows the characteristics of the nominal gain as a function of buckling angle, and the gain error, that is calculated gain differences between (6) and (7), corresponding to various $\Delta x/L$ ratio.

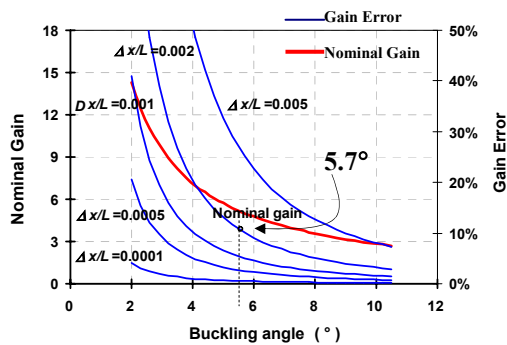


Figure 7. Nominal gain and gain errors as a function of buckling angle corresponding to different $\Delta x/L$ ratio.

The gain error is defined as the maximum discrepancy to the nominal gain. The gain error is an indicator for the nonlinearity as it is approximately twice of the nonlinearity determined experimentally. Once the device operating range ($\Delta x/L$) is specified, the nominal mechanical gain can be determined by the required linearity. For example, if the device is shooting for a range $\Delta x/L$ around 0.002 with gain error less than 10%, which results in a buckling angle of 5.7° , corresponding to a mechanical gain of 5, or differential mechanical gain of 10, with two sets of beams moving differentially.

Electronic linearity compensation

Based on the analysis, a 2nd order nonlinear electronic compensation method can be employed to achieve a much improved overall system linear performance. Fig. 8 shows an expected output of a linear capacitance to voltage converter (C/V) exhibiting a nonlinearity of 6% FS, along with an expected output from a 2nd order nonlinear compensated C/V achieving an improved nonlinearity of 0.22%. A 2nd order nonlinear C/V can be implemented by employing a linear C/V followed by a square-law amplifier, as shown in Fig. 9.

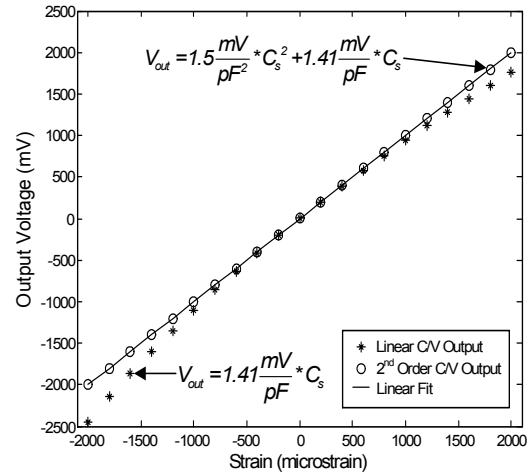


Figure 8. Simulation results with and without nonlinearity compensation.

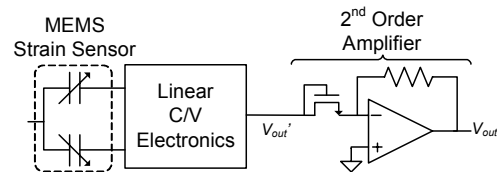


Figure 9. Proposed nonlinearity compensation architecture.

III. DEVICE DESIGN, FABRICATION, AND TESTING

The device fabrication process started with a SOI wafer with a device/oxide layer of 20/2 μm . The aluminum contact was first patterned, followed by DRIE to form the microstructure. A backside DRIE was used to generate the packaging frame, which also serves as a dicing step to avoid

contamination introduced by a saw dicing process. The oxide layer is then removed using dry etching to release the device. Fig. 10 presents an SEM picture of a fabricated sensor exhibiting a gauge length of 1000 μm , a buckling angle of 5.7° , a total number of 260 sensing fingers, and an air gap of 3.6 μm , as listed in TABLE I.

TABLE I. DEVICE PARAMETERS USED IN COUPLED-FILED FEA ANALYSIS

L_b	Buckling beam length (μm)	460
h	Buckling beam height (μm)	46
L_s	Central beam length (μm)	80
L_g	Gauge length (μm)	1000
α	Buckling angle	5.7°
$A_{mech\ nom}$	Nominal mechanical gain	5
W_f	Comb finger width	2.64 μm
g	Finger gap	3.36 μm
N_s	Number of fingers	260

The sensor was bonded on a stainless steel beam by using epoxy MB600[®] and tested on a three-point testing fixture. The mechanical gain was determined by analyzing the captured microscope finger movement images. The capacitance output was obtained by a calibrated capacitance-to-voltage conversion interface circuit (MS3110[®] from Microsensors). Fig. 11 shows a measured capacitance output characteristics. An overall sensor mechanical gain of 9.5 and a sensitivity of 210 aF/microstrain with nonlinearity of 6.8% over $\pm 2000 \mu\epsilon$ were achieved. Considering the applied strain range from -1000 to +1000 $\mu\epsilon$, the device demonstrated a much improved linearity performance from 5%, which is measured from the previous design to 1.2%. The measurements also match closely with the FEA modeling results with a maximum discrepancy less than 5%, as shown in Fig. 12, indicating the accuracy of the modeling.

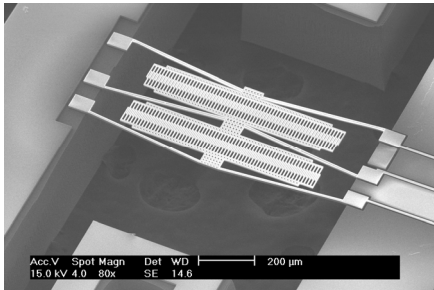


Figure 10. SEM picture of a fabricated device.

IV. CONCLUSION

The analysis, design, fabrication and evaluation of a mechanically amplified capacitive strain sensor are presented. In-depth analytical analysis is given to reveal the relationships between the mechanical gain, operation range, and linearity characteristics. Based on the analysis structure improvements and optimal parameters were achieved. The measurement results agree very well with the analysis results, which enables a nonlinear electronics linearity

compensation scheme. Simulation results show that, by applying this technique, the overall system nonlinearity can be greatly reduced from 6% FS to 0.2% FS.

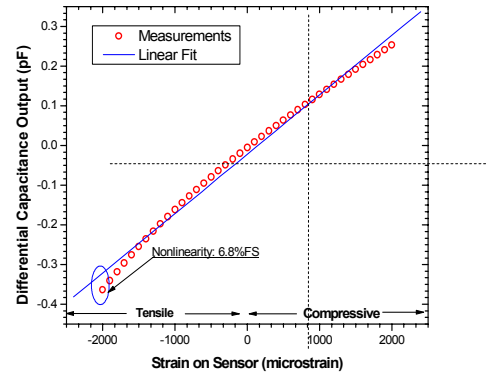


Figure 11. Measurement results.

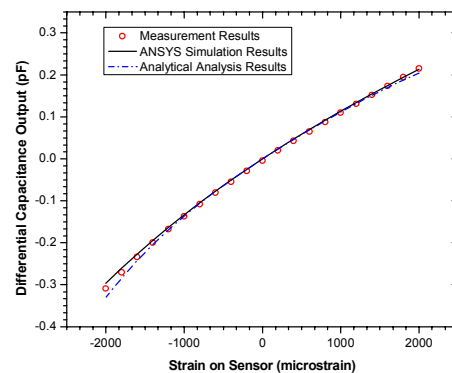


Figure 12. Comparison of sensor capacitance output characteristic obtained analytically, by FEA, and the measurements of a fabricated device.

ACKNOWLEDGMENT

This work is supported by U.S. Army Research Office (ARO) under contract #DADD19-02-1-0198.

REFERENCES

- [1] J. Guo, H. Kuo, D. J. Young and W. H. Ko, "Buckled beam linear output capacitive strain sensor." Solid-state Sensor, Actuator and Microsystems Workshop 2004 at Hilton Head, pp. 399-403, June 2004.
- [2] M. Suster, J. Guo, N. Chaimanonart, W. Ko, and D. Young, "Low-Noise CMOS integrated sensing electronics for capacitive MEMS strain sensors," IEEE Custom Integrated Circuits Conferenc, pp. 693-696, October 2004.
- [3] S. P. Timoshenko and S. woiniwsky-Krieger, "Theory of Plates and shells", 2nd edition, McGraw-Hill, 1970.
- [4] Yogesh B. Gianchandani and Khalil Najafi, "Bent-beam strain sensors", JMEMS, VOL. 5, No. 1, pp. 52-58, March 1996.